Supplemental Appendix

Expanded Methods

Patients and clinical specimens

The study was approved by the Ethical Committee of Shanghai Tenth People's Hospital. Fifteen patients were recruited at the Department of Cardiology, while 15 healthy individuals were recruited at the physical examination center from December 2018 to March 2019. All patients underwent laboratory examination and echocardiography (Supplemental Table 1). HCM was defined as wall thickness ≥ 15 mm in one or more left ventricular myocardial segments measured by echocardiography according to 2020 AHA/ACC guideline for the diagnosis of patients with HCM (1). Patients with a history of congenital heart disease, valvular heart disease, coronary artery disease, atrial fibrillation, drug-refractory hypertension, cancer and renal dysfunction were excluded from the study.

Human heart samples (3 cases) were collected from autopsied individuals died from heart failure in the pathology archives of the First Affiliated Hospital of Gannan Medical University between 2010 and 2016, while the control samples (3 cases) were collected from patients died of a non-cardiac reason.

The comparison of the baseline variables of interest were performed according to the patients with HCM or not. Continuous variables, such as age, EF, IVSd, LVPW and E/e', were denoted as mean ± standard deviation, and student's t test was conducted to compare the variables. Category variables, such as sex, were denoted as number (proportions) of male, and χ^2 test was conducted to compare the variables.

Animals

All experimental procedures involving animals were performed in accordance with the guidelines of the National Institutes of Health for the care and use of laboratory animals (NIH Publication, 8th Edition, 2011) and approved by the Animal Care and Use Committees of Shanghai Tenth People's Hospital.

Global *Nlrc5* knockout (KO) mice on C57BL/6J background were obtained from Shanghai Model Organisms Centre and bred as previously described (2). *Nlrc5*$^{flox/flox}$ mice were generated as described previously (3). Briefly, 5'loxP sites were inserted in the upstream of exons 1 where the promoter of EGE-LJL-121 was located. The 3'loxP was inserted into intron1 that was big and loxP element would not interfere mRNA splicing. To minimize the possibility of disruption of EGE-LJL-12 expression, two loxP sites were inserted into non-conserved regions. Southern blot and PCR were used by amplifying the region with the specific primers to identify the existence of loxP.

Transverse Aortic Constriction (TAC) surgery

The mice model of pressure overload-induced cardiac hypertrophy was created by transverse aortic constriction (TAC). Adult mice (C57BL/6J Background), weighing 20-25 g, were anaesthetized with amobarbital (60 mg/kg, intraperitoneal injection). The adequacy of anesthesia was judged by the absence

of withdrawal reflex to tail pinch. Mice were placed in the supine position. Chest was opened to identify the thoracic aorta. A 6-0 silk suture was placed through below the transverse aorta and tied around a 27-gauge blunt needle which was subsequently removed. Sham mice underwent the same procedure without the aortic constriction. After 4 weeks, survived animals were analyzed with echocardiography and then killed by cervical dislocation.

Echocardiography and blood pressure measurements

Mice were anesthetized with 2.5% isoflurane and then maintained at 1.0-1.5%. Anesthetized mice underwent transthoracic echocardiography using a Vevo2100 ultrasound system (Visual Sonics; Toronto, Canada). Repeated measurements were performed at baseline, 1- and 4-weeks post-surgery. Hearts were viewed in the short-axis at the level of the midpapillary muscles for M-mode. Fractional shortening (FS), ejection fraction (EF), left ventricular internal diameter at end-systole (LVIDs), left ventricular posterior wall diameter at end-systole (LVPWs) and left ventricular (LV) mass were calculated from M-mode measurements automatically. Images were acquired in the short-axis B-mode and M-mode for analysis of cardiac function and dimensions. Pulse wave Doppler echocardiography (ECHO) of the transverse aorta was used to measure the peak pressure gradients at the aortic constriction (Supplemental Figure 4E, 8J to 8K, 14F). Mice with a maximum peak gradient of less than 40 at 1-week post-surgery were excluded from the study. ECHO data shown in this study come from animals that received baseline and 1 week ECHO.

Arterial blood pressure (BP) was measured by the mouse-tail cuff method using the automated BP-2000 Blood Pressure Analysis System (Visitech Systems, USA). In brief, mice were acclimated to the procedure for 3 days before measurements to avoid undue stress and experimental artifact. After training, BP was measured one day before treatment to determine the baseline BP values in each mouse cohort. BP and heart rate measurements were carried out at the same time in a predetermined quiet area. Measurements were repeated several times during experiments. Fifteen consecutive systolic and diastolic BP measurements were made, and the last 10 readings per mouse were recorded and averaged.

Flow cytometry

Peripheral blood cells from each mouse were obtained using heparin anticoagulant tubes before harvesting heart tissues. Hearts were then perfused with ice-cold PBS thoroughly and chopped finely and digested, while shaking, for 1 hour at 37°C in HBSS containing collagenase I (450 U/mL), DNase I (60 U/mL) and hyaluronidase (60 U/mL) enzymes (all Sigma, USA). The digested material from heart was filtered through 70 μm filters and pelleted by centrifugation (400 x*g* for 5 minutes at 4°C) in HBSS supplemented with 2% FBS and 0.2% BSA. Red blood cells were lysed in 10 × FACS Lysing Solution (BD Pharmingen, USA) for 5 min at room temperature and resuspended in FACS buffer (PBS containing 2% FBS and 2mM EDTA). Gating strategies with isotype controls for macrophages, neutrophils, monocytes and T cells were shown in Supplemental Figure 6.

Histology and immunohistology

For histological analysis, heart tissue samples were fixed in 10% formalin, dehydrated, and paraffin-embedded for sectioning into 5-μm-thick sections and then used for hematoxylin eosin staining (HE), Masson's staining and immunohistochemical staining.

For immunohistochemistry staining, sections were treated with microwave-based antigen retrieval using 10 mM sodium citrate buffer and then incubated with 0.3% hydrogen peroxide for 10 minutes to inactivate endogenous peroxide activity. After three washes in phosphate-buffered saline (PBS) and being blocked in 10% goat serum for 30 minutes at room temperature, sections were incubated at 4 °C overnight with primary antibodies, including anti-NLRC5 (ab105411, Abcam, USA), anti-Fibronectin (sc8422, Santa Cruz, USA) and anti-Collagen I (ab270993, Abcam, USA). A standard ABC-peroxidase system (Vector Laboratories, USA) was used to detect primary antibodies. Positive antibody binding was visualized using a DAB peroxidase substrate kit (SK-4100, Vector Laboratories, USA). Normal isotype-matched IgG (sc2025 and sc2027, Santa Cruz, USA) was used as negative control. ImageJ software (V1.49, NIH, USA) was used for image analysis. NLRC5-, Collagen I- and Fibronectin-positive signals within selected heart tissues were determined semi-quantitatively and expressed as the percentage of the positive area within the entire hearts.

Immunofluorescence staining and confocal microscopy

Cells were seeded at 1×10^5 cells/well on glass-bottomed culture dishes and then fixed with freshly prepared 4% paraformaldehyde for 15 minutes, followed by permeabilization with 0.2% Triton X-100 in PBS for 5 minutes. Human or mouse heart tissues were harvested and processed in optimal cutting temperature compound and sliced into 5 μm-thick sections. Paraformaldehyde-fixed sections, cryosections, and cells were incubated with anti-NLRC5 (ab105411, Abcam, USA), anti-α-smooth muscle actin (α-SMA, ab7817, Abcam, USA), anti-Mac2 (14-5301-81, Invitrogen, USA), anti-CD68 (14-0681-80, Invitrogen, USA), anti-Troponin T (MA5-12960, Invitrogen, USA), anti-α actinin 4 (ab32816, Abcam, USA), anti-CD31 (557355, BD Bioscience, USA), anti-HSPA8 (sc7298, Santa Cruz, USA), anti-Ly6G (127601, BioLegend, USA), anti-CD3 (14-0031-82, Invitrogen, USA) overnight at 4 °C. Normal isotype IgG (sc2025, sc2026, and sc2027, Santa Cruz, USA; 14-4888-81, Invitrogen, USA) was used as negative control (Supplemental Figure 2A). Mouse spleen tissues were used as positive controls for labeling NLRC5 and CD68 (Supplemental Figure 2B). Human lung tissues were used as positive controls for labeling NLRC5 and CD68 (Supplemental Figure 2B). After washing with PBS, secondary antibodies including Alexa Fluor 594-conjugated goat anti-rabbit, Alexa Fluor 594-conjugated goat anti-mouse, Alexa Fluor 488-conjugated goat anti-rat, Alexa Fluor 488-conjugated goat anti-Armenian hamster, Alexa Fluor 488-conjugated goat anti-mouse, and Alexa Fluor 647-conjugated goat anti-rat (Thermo Fisher Scientific, USA) were incubated for 1 hour at 37 °C in the dark. To analyze cardiomyocyte size, sections were incubated with wheat germ agglutinin (WGA, W32466, Thermo Fisher Scientific, USA) at room temperature for 30 minutes. Nuclei were labeled with DAPI (Vector Laboratories, USA). Images were collected using a Nikon A1R confocal microscope system equipped with a Nikon Eclipse Ti-E inverted microscope, running NIS Elements

software (Nikon Instruments, USA). Mean cardiomyocyte cross-sectional area was measured in transverse sections stained with α-actinin or WGA used by Image J software. The values of at least 100 cell areas in each group were integrated into the final statistical mapping.

Cell lines

HEK293T, H9C2 and RAW264.7 were obtained from were purchased from Fudan University Institutes of Biomedical Sciences Cell Center (Shanghai, China). The cells were cultured in DMEM supplemented with 10% heat-inactivated FBS, 1% penicillin/streptomycin. All cell lines were kept in an incubator at 37°C with 5% CO2 and 95% relative humidity.

Generation of bone marrow derived macrophages and peritoneal macrophages

Total bone marrow cells were harvested from femur bones into the DMEM. Cell suspension was filtered through a 70 mm nylon strainer into a 50 mL tube. Then the tube was centrifuged at 1500 rpm for 10 min at 4°C. The cell pellet was washed and resuspended in DMEM supplemented with 10% FBS (fetal bovine serum), 40ng/ml M-CSF (macrophage colony-stimulation factor, PeproTech, cat# AF-315-02) and 1% penicillin/streptomycin. The cells were then plated in a sterile six-well tissue culture plate, and cultured for 7 days. At day 3, a half volume of fresh DMEM with 10% FBS and 40ng/ml M-CSF was added.

For peritoneal macrophages culture, mice were injected intraperitoneally with 1.5 ml 3% (w/v) thioglycolate medium (BD Biosciences), and primary macrophages were isolated 3–4 days later by flushing with ice-cold 1 × PBS buffer. Cells were seeded at a density of 3×10^6 cells per well in DMEM supplemented with 10%FBS and 1% penicillin/streptomycin, and maintained at 5% CO_2 at 37 °C. After overnight culture, cells were washed twice with medium to remove nonadherent cells.

Cell isolation from tissue samples

Neonatal rat cardiomyocytes (CMs) and cardiac fibroblasts (CFs) were isolated from 0-3-day-old Sprague Dawley rats. In brief, pups were placed on ice for 5-10 minutes for light anesthesia. After decapitation, hearts were collected, the atria were carefully removed, and the blood washed away. The ventricles were minced and digested in 1 mg/ml collagenases type II solution in a 37°C water bath pot, shaking gently. Every 10 minutes the solution containing the digested cells was transferred to a new tube containing FBS (Gibco, USA). The remaining not dissociated tissue residue was supplemented with fresh enzymatic solution for additional five times. The supernatant was centrifuged for 5 minutes (400 x g) and resuspended in HBSS supplemented with 20% FBS. To remove any contaminating fibroblasts, collected cells were seeded onto uncoated 100 mm plastic dishes for 1 hour at 37 °C in 5% CO_2 humidified atmosphere. The supernatant, which consists mainly of CMs, was collected and cells were counted and plated on gelatinized 6 well plates 1×10^6 cells per well. The medium consisted of DMEM/F12 medium (HyClone, USA) supplemented with 20% FBS and 1% penicillin/streptomycin. This procedure yields > 90% pure CMs. For CF culture, the supernatant was centrifuged for 5 minutes (400 x g), resuspended in DMEM medium

supplemented with 10% FBS and plated on 6 well plates. The peripheral blood neutrophils (PMNs) were isolated by differential centrifugation. T cells were purified from spleen cells by negative selection using the Pan T Cell Isolation Kit (Miltenyi Biotec, Germany). B cells and T cells were isolated from mouse spleen using mouse B cell and Pan T cell isolation kits (Miltenyi Biotech, Germany) according to manufacturer's instruction.

Adenovirus infection, plasmid transfection and small interfering RNA (siRNA) transfection

Bone marrow-derived macrophages (BMDMs) and RAW264.7 cells were seeded in 6-well-plates or 100mm dishes over 70% confluence and used for *in vitro* adenovirus infection. The Flag-tagged NLRC5 (Ad-Flag-NLRC5) and control adenovirus (Ad-Control), which were constructed and purchased from Shanghai Genechem Co., Ltd, were added into the serum-free medium at the concentration of 50 mM for 24 hours. The medium was replaced by the complete medium for another 24 hours and used for further experiments. Myc-HSPA8 plasmids were constructed and purchased from Shanghai Genechem Co., Ltd. Myc-HSPA8 and control plasmids were generated from pGV658 vector with Myc tag. Transfection of the RAW264.7 and HEK293T cells was performed with jetOPTIMUS (Polyplus-transfection, France) and Lipofectamine 2000 (Invitrogen, USA) respectively according to the manufacturer's instructions. The duplex siRNA targeting HSPA8 (siHSPA8) and scramble siRNA (siCtr) were purchased from GENECHEM Biotech (GENECHEM, China). BMDMs were transfected with 50 nM siRNA using of INTERFERin (Polyplus-transfection, France) for 24 h.

Mass spectrometry

Protein was extracted from bone marrow-derived macrophages (BMDMs) transfected with Ad-Control or Ad-Flag-NLRC5. NLRC5 was immunoprecipitated from Ad-Flag-NLRC5-transfected BMDMs using monoclonal Flag antibody (14793S, Cell Signaling Technology, USA). Immunoprecipitants were separated by SDS-PAGE and stained with the Colloidal Blue Staining kit (Beyotime, China). Liquid chromatography-tandem mass spectrometry/mass spectrometry (LC-MS/MS) analysis was performed on an EASY-nLC 1200 ultra-high-pressure system combined with Q Exactive Plus high-resolution mass spectrometer via a nano-electrospray ion source (all from Thermo Fisher Scientific, USA) at Shanghai OE Biotech Co., Ltd. The data were searched against a Uniprot Mus musculus database with Proteome Discoverer 2.4 (Thermo Fisher Scientific, USA). Proteins and peptides with a false discovery rate (FDR) of 1 % were selected.

RNA sequencing

BMDMs were transfected with Ad-Control and Ad-Flag-NLRC5 (50 MOI) for 24 hours. Then, HSPA8 knockdown (siHSPA8, GENECHEM, China) and control treatment (siCtr) were used to stimulate BMDMs for another 24 hours. RNA sequencing was conducted with the help of OE Biotech Co., Ltd (China). Briefly, RNA was harvested using Trizol reagent, Illumina TruSeq RNA Sample Prep Kit (Cat# FC-122-1001) was used with 1 μg of total RNA for the construction of sequencing libraries. RNA libraries were prepared for sequencing using standard Illumina protocols, and RNA sequencing was subsequently performed using the

Illumina NovaSeq 6000 platform. Finally, differentially expressed genes were screened using DESeq (version 1.22.1). Raw and processed data were deposited in SRA (accession PRJNA754868)

GSVA analysis

To explore the underlying changes in pathway activity between two groups with significant differences, we performed Gene set variation analysis (GSVA) to calculate the scores for each group based on previously defined gene sets of KEGG pathways. Enriched gene sets were assigned based on control P-value < 0.05 as significantly altered.

Fluorescence-activated and Magnetic-activated cell sorting

$CD14^+$ monocytes, $CD16^+$ neutrophils, $CD3^+$ T lymphocytes and $CD19^+$ B lymphocytes were isolated from human peripheral blood cells using a MACS system (Miltenyi Biotec, Germany). For each volunteer, 9 ml of venous blood was diluted with an equal volume of 1 x PBS (HyClone, USA). The diluted blood was then carefully layered onto 7.5 ml of Ficoll-Paque Plus solution (GE Healthcare, USA) and centrifuged for 25 minutes at 400 ×*g* (without acceleration and brake). After centrifugation, peripheral blood mononuclear cells (PBMCs) in the middle layer were collected and washed twice with 10 ml of 1× PBS. Granulocytes in the lowest layer were collected after erythrocytes were lysed. Then mononuclear cells were labeled with CD14, CD3 and CD19 MicroBeads separately and granulocytes were labeled with CD16 MicroBeads (Miltenyi Biotec, Germany). MS MACS columns and a MACS Separator (Miltenyi Biotec, Germany) were used to isolate monocytes, neutrophils, T lymphocytes and B lymphocytes respectively. The efficiency of MACS was further confirmed by flow cytometry (Supplemental Figure 1D).

For isolation of $F4/80^+$ macrophages in hearts, heart tissues were collected into cold MACS buffer and carefully cut into small fragments (1-2 mm), followed with mechanical disruption using C-tubes (Miltenyi Biotec, Germany) and GentleMACS dissociator (Miltenyi Biotec, Germany) with the program Multi D. The disrupted heart tissues were continuously rotated at 37°C for 15 minutes and subjected to GentleMACS dissociator using the program Multi C. Each heart was digested with 2.5 ml in-house digestion buffer consisting of 0.76 U/ml Liberase TL (Sigma-Aldrich, USA) and 2mg/ml DNase I (Roche, USA) dissolved in HBSS with Ca^{2+} and Mg^{2+} (HyClone, USA). Cells released during enzymatic digestion were filtered through Falcon 40 μm cell strainers, and red blood cells were lysed with Pharm Lyse Buffer (BD Biosciences). Isolated heart cells were labeled with F4/80 MicroBeads (Miltenyi Biotec, Germany) and macrophages were isolated by magnetic separation with MS MACS columns and a MACS Separator.

All isolated cells were subjected to mRNA extraction by RNAprep Pure Micro Kit (TIANGEN, China), prepared for subsequent RT-PCR analysis.

For fluorescence-activated cell sorting (FACS), the single-cell suspension of human PBMCs was incubated with anti-CD45-BV421, anti-CD14-APC and anti-CD16-PE antibodies (1:200, BioLegend, USA) for 30 minutes on ice. After incubation, cells were washed and resuspended in FACS buffer. FACS was conducted using a BD FACS Aria II (BD Biosciences, USA). FACS strategy is shown in Supplemental

Figure 1C. FACS-sorted classical monocytes ($CD14^{++}CD16^{-}$) , intermediate ($CD14^{++}CD16^{+}$) and non-classical ($CD14^{+}CD16^{++}$) monocytes were collected in 1.5 ml Eppendorf tubes containing buffer RL (RNAprep Pure Micro Kit, TIANGEN, China), which were subjected to mRNA extraction and complementary RT-PCR analysis.

RNA extraction and quantitative real-time PCR

The total RNA was extracted using Trizol reagent (Thermo Fisher Scientific, USA). In all, 1000 ng of total RNA was reversely transcribed to cDNA using PrimerScript RT Reagent Kit (Vazyme, China). Quantitative real-time PCR was performed with a LightCycler 96 PCR (Roche, USA) with a 20 μL SYBR Green reaction system (Vazyme, China). PCR amplification was performed for 40 cycles. The expression of housekeeping gene (*GAPDH)* was employed to normalize gene expression levels. The primer sequences are listed in Supplemental Table 3.

Protein extraction and western blot

Heart tissue lysate and whole cells from *in vitro* experiments were prepared by 1× cell lysis buffer (Cell Signaling Technologies, USA) containing protease inhibitors (Roche, USA). Supernatant proteins were concentrated with equal methanol and a quarter of trichloromethane. Proteins were separated by SDS-PAGE and transferred to polyvinylidene fluoride (PVDF) membranes. After blocking in 5% nonfat milk for 1 hour at room temperature, PVDF membranes were incubated overnight at 4°C with primary antibodies including anti-NLRC5 (sc515668, Santa Cruz, USA), anti-ANP (ab91250, Abcam, USA), anti-HSPA8 (ab51052, Abcam, USA), anti-IKKβ (8943S, Cell Signaling Technology, USA), anti-p-IKKβ (ab194519, Abcam, USA), anti-p38 (8690S, Cell Signaling Technology, USA), anti-p-p38 (4511S, Cell Signaling Technology, USA), anti-STAT3 (9139S, Cell Signaling Technology, USA), anti-p-STAT3 (9145S, Cell Signaling Technology, USA), anti-pro-IL-1β+IL-1β (ab234437, Abcam, USA), anti-pro-Caspase-1+Caspase-1 (ab179515, Abcam, USA), anti-GAPDH (Proteintech, USA, 1:5000), anti-Flag (14793S, Cell Signaling Technology, USA), and anti-Myc (2272S, Cell Signaling Technology, USA). Primary antibodies were then incubated with secondary antibody for 1 hour and bends were visualized using chemiluminescence (ECL; TANON, China) and viewed under Amersham Imager 600 system (GE Healthcare, USA).

Immunoprecipitation

Macrophages or HEK293T cells were lysed in lysis buffer (Cell Signaling Technologies, USA) with phenylmethylsulfonyl fluoride (PMSF) (Roche, USA) and protease inhibitor cocktail (Roche, USA) on ice for 20 minutes. Lysate was cleared by centrifugation at 12,000 rpm at 4°C for 15 minutes to obtain the cell extracts. After centrifugation, 500 μg of cell lysate was incubated with 5 μg of the indicated primary antibodies at 4 ℃ overnight. The lysate immunoprecipitated with anti-IgG served as negative control. The immune complexes were then purified by 20 μl of protein A/G agarose (Santa Cruz, USA) at 4 ℃ for 3 hours, centrifuged and washed by ice-cold cell lysis buffer. The immunoprecipitated protein was separated

by SDS-PAGE using 8% or 10% gels followed by western blots. Immunoblot data were quantified and analyzed with ImageJ software (V1.49, NIH, USA).

Bone marrow transplantation (WT to WT/KO)

Recipient mice were irradiated with 9 Gy of radiation at least 6 hours prior to injection. On the day of bone marrow transplantation, donors were sacrificed and disinfected. Femur and tibia were collected in sterilized PBS on ice, and muscle tissue was thoroughly cleaned. Both ends of the bones were cut off and bone marrow cells were flushed out using 1 ml syringe needle filled with RPMI-1640 medium. Bone marrow was filtrated through 0.45 μm strainer. Cells were centrifuged and then suspended with 1 ml RPMI-1640. After being counted, cells were transplanted to recipients through tail vein injection. Each recipient was injected with 1×10^7 cells with an injection volume of 400 μl.

Cytokine profiling array

Thirty-six different inflammatory markers of BMDMs at the proteins level were examined using Mouse Cytokine Array (R&D System, USA) according to the manufacturer's instructions. Briefly, membranes were incubated with 1 ml culture medium of BMDMs and a cocktail of biotinylated antibodies overnight at 4 °C. Following three washes, membranes were incubated in the presence of 2 ml (1:2000 dilution) of streptavidin–horseradish peroxidase for 30 minutes at room temperature, and the presence of immunocomplexes was detected by staining with 3, 3′-diaminobenzidine chromogen. Arrays were scanned and pixel density was quantified using ImageJ software (V1.49, NIH, USA).

ELISA for IL-6 was measured in BALF and serum samples using an ELISA kit according to the manufacturers protocol (R&D Systems, USA). The detection limit for IL-6 was 2 pg/ml. The homogenization buffer was tested as a negative control.

Cell proliferation analysis assay

Cell proliferation was analyzed using the CCK8 proliferation method (Yeasen, China). In brief, 1×10^4 cells/well were seeded in triplicate in 96-well plates and incubated at 37°C and a 5% CO_2 humidified atmosphere. After 24, 48 and 72 hours, the CCK8 assay was performed according to the manufacturer's protocol. All experiments were performed in triplicate. Viable cells were counted by absorbance measurements at 450 nm using SpectraMax i3 Multi-Mode Microplate Detection Platform (Molecular Devices, USA).

EdU was added to culture media at 10 μM final concentration for 24 hours. Following cell fixation, EdU was labeled using Click-iT EdU Alexa Fluor 594 Imaging Kit (Thermo Fisher Scientific, USA). Cells were imaged on a Zeiss LSM700 at 20× and images were analyzed using ImageJ. Data shown represents six subclones.

Supplemental References

1. Ommen SR, et al. 2020 AHA/ACC Guideline for the Diagnosis and Treatment of Patients With Hypertrophic Cardiomyopathy: Executive Summary: A Report of the American College of Cardiology/American Heart Association Joint Committee on Clinical Practice Guidelines. *J Am Coll Cardiol.* 2020;76(25):e159-e240.
2. Luan P, et al. NLRC5 inhibits neointima formation following vascular injury and directly interacts with PPARgamma. *Nat Commun.* 2019;10(1):2882.
3. Xu X, et al. The subcellular redistribution of NLRC5 promotes angiogenesis via interacting with STAT3 in endothelial cells. *Theranostics.* 2021;11(9):4483-501.

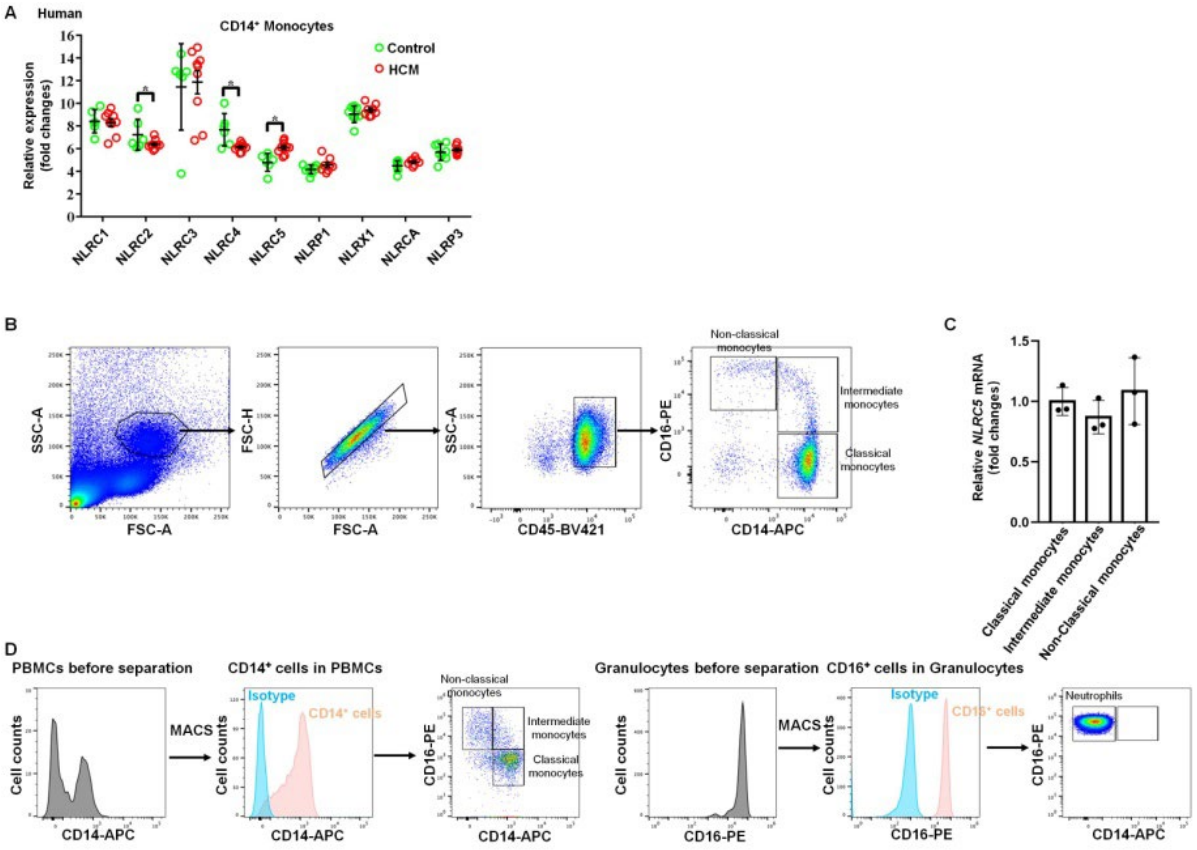

Supplemental Figure 1 NLRC5 expression in CD14$^+$ monocytes from controls and HCM patients. (**A**) Relative mRNA expression of some NLR family members including *NLRC1, NLRC2, NLRC3, NLRC4, NLRC5, NLRP1, NLRX1, NLRCA* and *NLRP3* in CD14$^+$ monocytes isolated from peripheral blood of hypertrophic cardiomyopathy (HCM) patients and controls. (**B**) Gating strategy for fluorescence-activated cell sorting (FACS) of monocyte subsets from human PBMCs. (**C**) The mRNA expression of *NLRC5* in classical, intermediate and non-classical monocytes was quantified by real-time PCR (n = 3 per group). (**D**) The magnetic-activated cell sorting (MACS) enrichments of monocytes and neutrophils from human peripheral blood were verified by flow cytometry. Data are expressed as mean ± SD. **P*<0.05. Data in panel (**A**) was analyzed using Student's unpaired *t*-test. Data in panel (**C**) was analyzed using Kruskal–Wallis followed by Dunn's multiple comparison test.

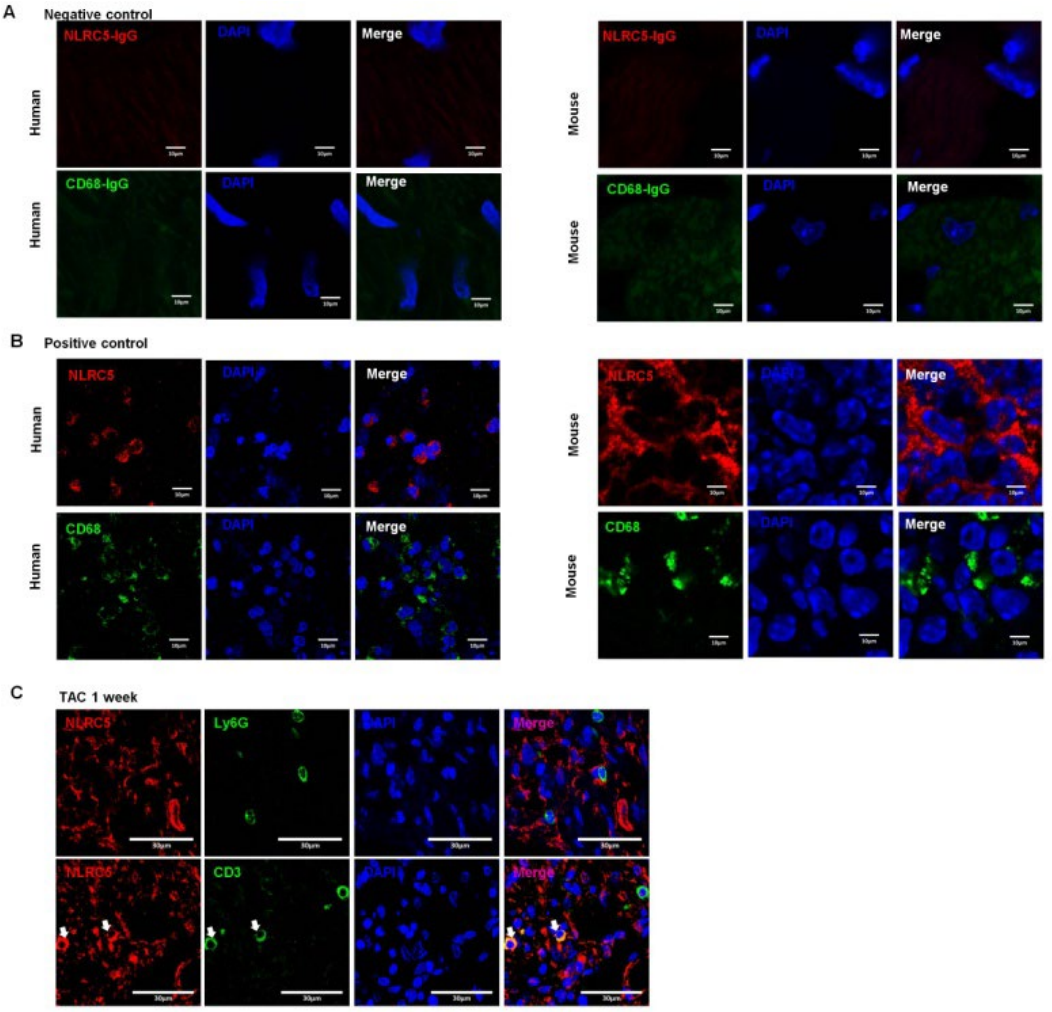

Supplemental Figure 2 NLRC5 expression in neutrophils and T lymphocytes located in hearts after TAC operation. (**A**) Negative control for immunofluorescence staining of NLRC5 and CD68 in heart sections with isotype IgG antibodies. Scale bars, 10 μm. (**B**) Human lung tissues and mouse spleen tissues were used as positive control for immunofluorescence staining of NLRC5 and CD68. Scale bars, 10 μm. (**C**) Immunofluorescence staining showed that NLRC5 (stained in red) was constitutively co-localized with neutrophils (labeled with Ly6G in green) and was rarely expressed in T lymphocytes (labeled with CD3 in green) in hearts after 1 week of transverse aortic constriction (TAC) operation. Scale bars, 30 μm.

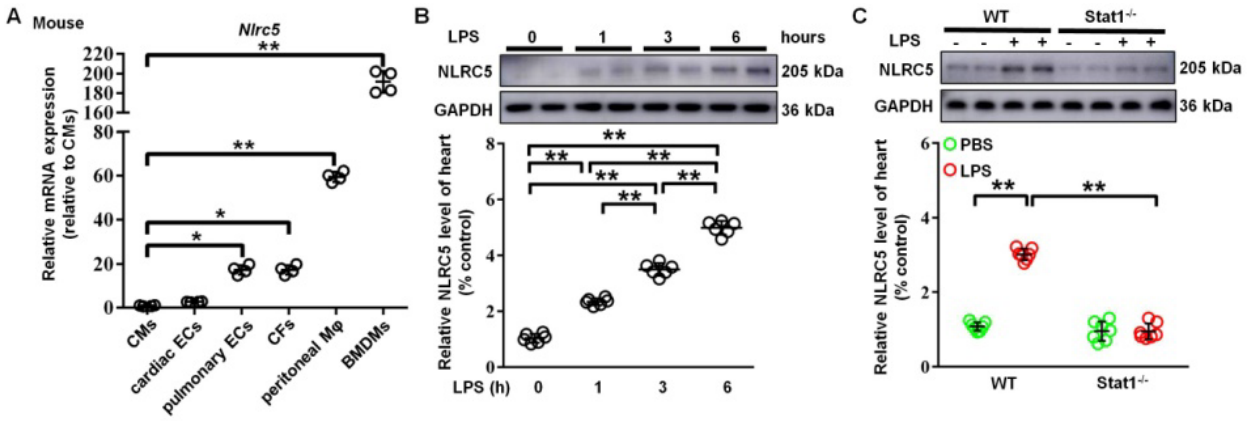

Supplemental Figure 3 LPS activated *NLRC5* expression through STAT1 pathway in BMDMs. (**A**) NLRC5 expression in different cell types. The mRNA expression of *Nlrc5* in cardiomyocytes (CMs), cardiac endothelial cells (ECs), pulmonary ECs, cardiac fibroblast (CFs), peritoneal macrophages (Mφ) and bone marrow-derived macrophages (BMDMs) was quantified by real-time PCR (n = 4 per group). The protein expression of NLRC5 was analyzed in BMDMs after 1, 3 and 6 hours of LPS treatment (**B**) and in WT or Stat1$^{-/-}$ BMDMs with or without LPS treatment (**C**) (n = 6-8 per group). Data are expressed as mean ± SD. *P<0.05, **P<0.01. Data in panel (**B**) was analyzed using repeated measures ANOVA. Other data was analyzed using one-way ANOVA followed by Tukey's post-hoc analysis.

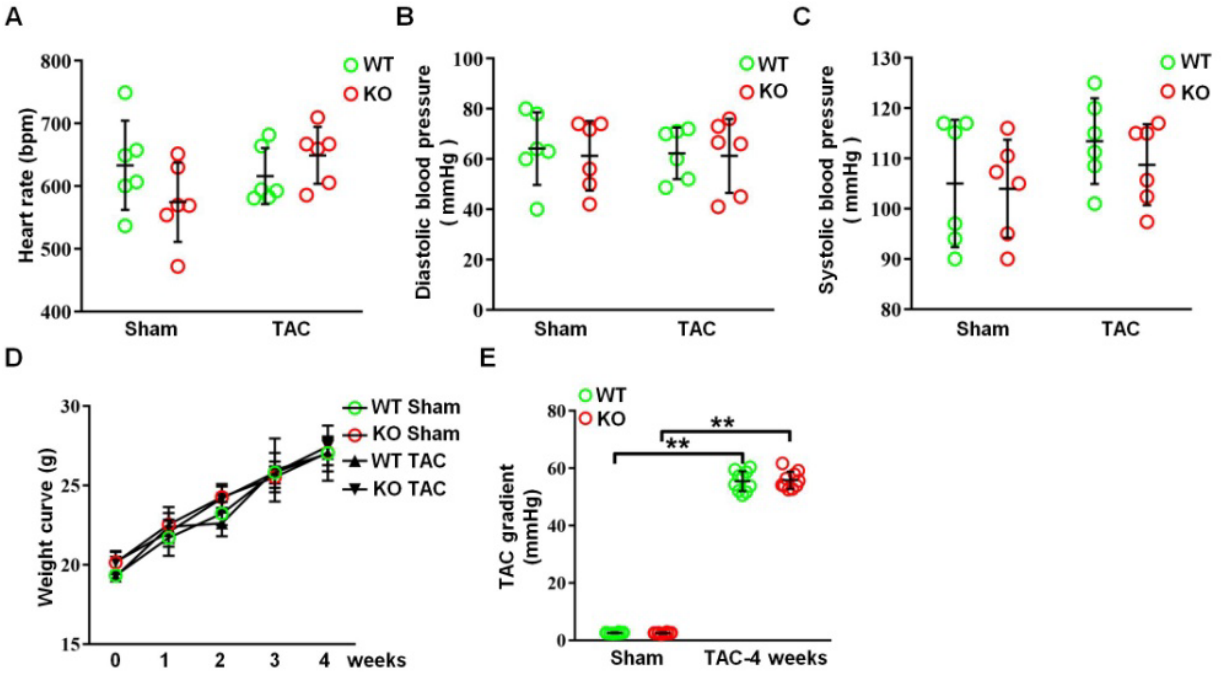

Supplemental Figure 4 Heart rate, noninvasive blood pressure and aortic gradient in WT and KO mice. (**A**) The heart rate of wild-type (WT) and *Nlrc5* knockout (KO) mice after 4 weeks of TAC (n = 6 per group). (**B, C**) The diastolic blood pressure and systolic blood pressure of WT and KO mice after 4 weeks of TAC (n = 6 per group). (**D**) The weight change curve of the WT and KO mice after 0, 1, 2, 3 and 4 weeks with TAC operation. (**E**) Peak pressure gradient across the aortic constriction was measured by Doppler after 4 weeks of TAC operation (n=10 per group). Data are expressed as mean ± SD. Data in panel (**B**) was analyzed using Kruskal–Wallis followed by Dunn's multiple comparison test. Other data were analyzed using one-way ANOVA followed by Tukey's post-hoc analysis.

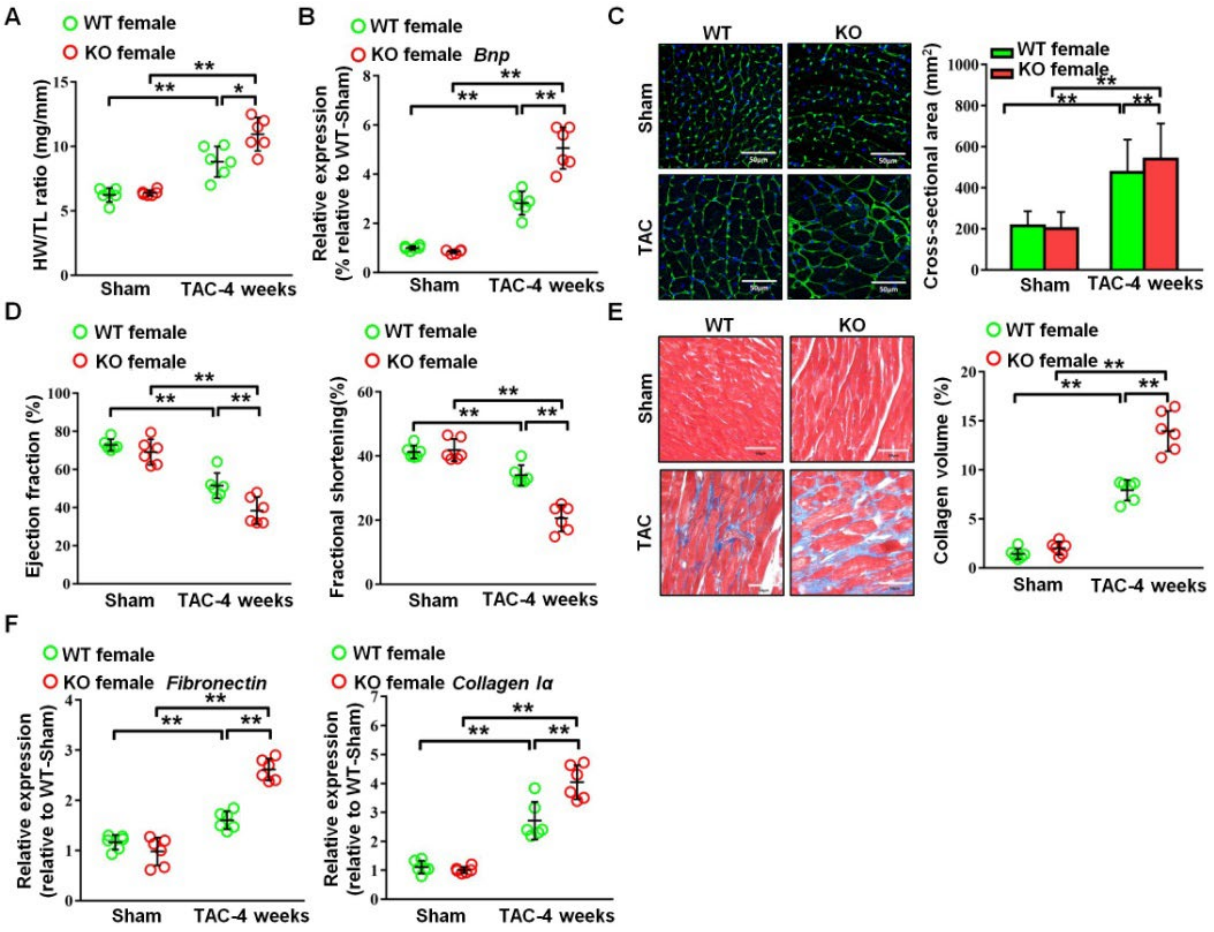

Supplemental Figure 5 NLRC5 deletion promoted cardiac remodeling induced by pressure overload in female mice. (**A**) The ratios of heart weight and tibia length (HW/TL) in WT and KO female mice (n = 6 per group). (**B**) Relative mRNA expression of cardiac hypertrophy-related markers *Bnp* was assessed (n = 6 per group). (**C**) Histological analysis of CM area was measured by wheat germ-agglutinin (WGA) staining. Scale bars, 50μm. (**D**) Echocardiographic analyses of ejection fraction (EF), fractional shorting (FS) after 4 weeks of TAC operation (n = 6 per group). (**E**) Representative Masson's trichrome staining and quantitative analysis of collagen volume of hearts from WT and KO female mice after sham or TAC operation (n = 6 per group). Scale bars, 50μm. (**F**) Relative mRNA expression of cardiac fibrosis markers *Fibronectin* and *Collagen Iα* was measured in heart tissues from WT and KO female mice with sham or TAC operation (n = 6 per group). Data were expressed as mean ± SD. *P<0.05, **P<0.01. Data were analyzed using one-way ANOVA followed by Tukey's post-hoc analysis.

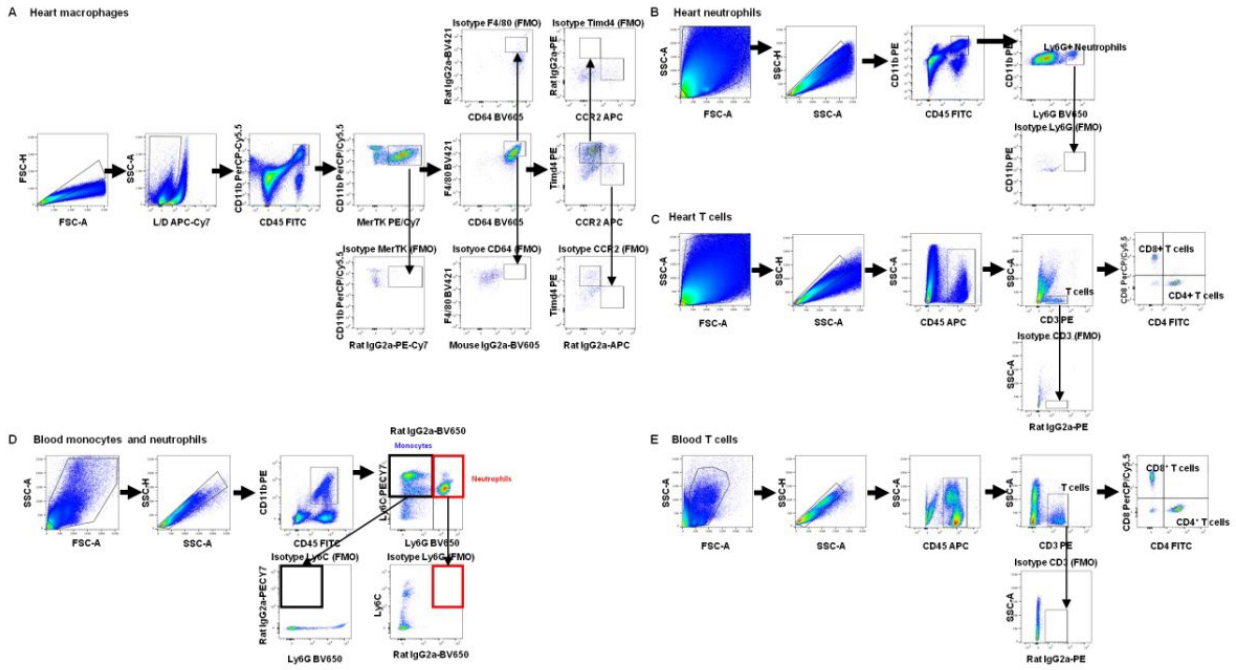

Supplemental Figure 6 Gating strategy for immune cells in heart and blood. (**A**) Cardiac Macrophages were identified as $CD45^{+}CD11b^{+}MerTK^{+}CD64^{+}F4/80^{+}$ cells by flow cytometry, resident macrophages were further identified as $CCR2^{-}Timd4^{+}$ while infiltrating cells were identified as $CCR2^{+}Timd4^{-}$. (**B, D**) Monocytes in blood were identified as $CD45^{+}CD11b^{+}Ly6G^{-}Ly6C^{+}$ cells and neutrophils in heart and blood were identified as $CD45^{+}CD11b^{+}Ly6G^{+}$ cells. T cells in heart (**C**) and blood (**E**) were identified as $CD45^{+}CD3^{+}$ cells and further subdivided into $CD4^{+}CD8^{-}$ T cells and $CD4^{-}CD8^{+}$ T cells. All isotype controls were presented in Fluorescence-Minus-One (FMO) gate.

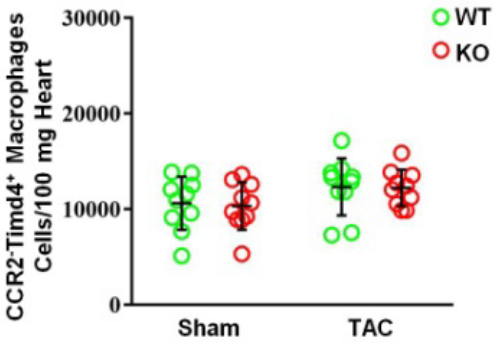

Supplemental Figure 7 Quantitative analysis of CCR2^{-}Timd4^{+}macrophages in heart tissues of WT and KO mice after 1 week of TAC (n = 10 per group). Data are expressed as mean ± SD. **P*<0.05, ***P*<0.01. Data was analyzed using one-way ANOVA followed by Tukey's post-hoc analysis.

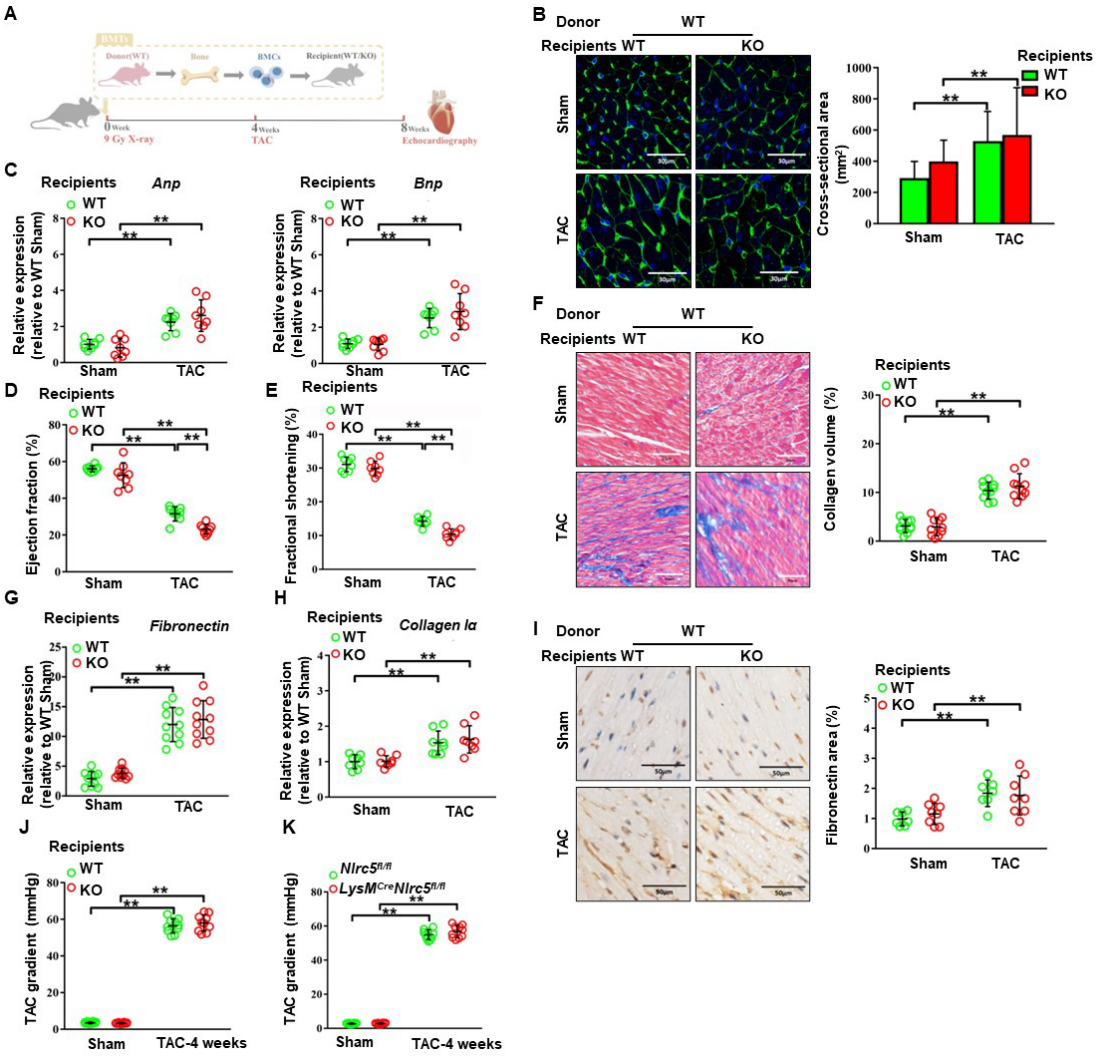

Supplemental Figure 8 BM transplantation indicated that deficiency of NLRC5 in non-BM-derived cells did not affect cardiac remodeling. (**A**) Experimental design. Both WT and KO recipient mice were transplanted with bone marrow (BM) from WT donor mice. After 4 weeks of BM transplantation, the chimeric mice were operated with TAC. (**B**) Representative images and quantitative analysis of transverse area of CMs detected by wheat germ-agglutinin (WGA) staining (n = 10 per group). Scale bars, 30μm. (**C**) Relative mRNA expression of *Anp* and *Bnp* were assessed in heart tissues, normalized to *Gapdh* (n = 8 per group). (**D, E**) Echocardiographic analyses of ejection fraction (EF) and fractional shorting (FS) after 4 weeks of sham and TAC operation (n = 8 per group). (**F**) Representative Masson's trichrome staining and quantitative analysis of hearts from WT and KO recipient mice with sham or TAC operation (n = 8 per group). Scale bars, 50μm. (**G, H**) Relative mRNA expression of cardiac fibrosis markers *Fibronectin* (**G**) and *Collagen Iα* (**H**) was measured by real-time PCR in heart tissues, normalized to *Gapdh* (n = 8 per group). (**I**) Immunohistochemistry staining and quantitative analysis of cardiac fibrosis reflected by Fibronectin in WT and KO recipient mice with sham or TAC operation (n = 8 per group). Scale bars, 50 μm. (**J, K**) Peak pressure gradient across the aortic constriction was measured after 4 weeks of sham or TAC surgery (n=10 per group). Data are expressed as mean ± SD. **P*<0.05, ***P*<0.01. Data was analyzed using one-way ANOVA followed by Tukey's post-hoc analysis.

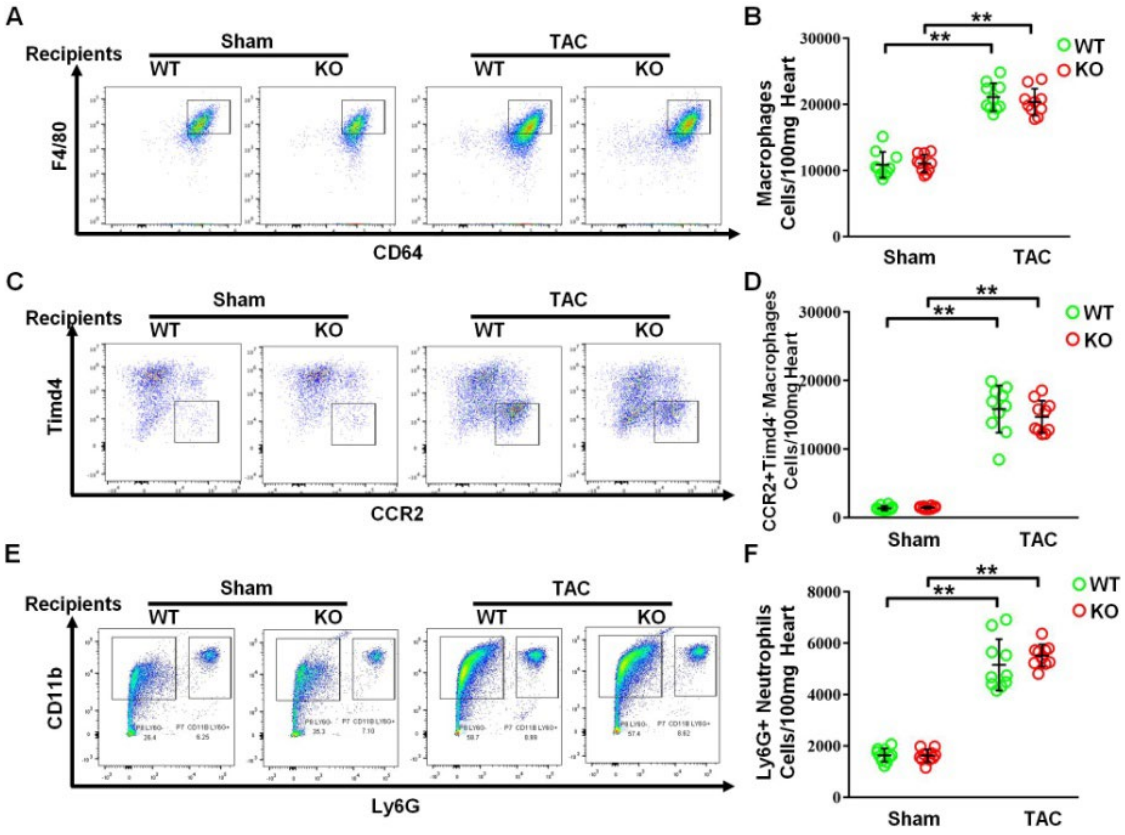

Supplemental Figure 9 The number of myeloid cells in hearts from WT and KO recipient mice with sham or TAC operation. (**A, B**) Representative cytograms and quantitative analysis of MerTK^{+}CD64^{+}F4/80^{+} macrophages in heart tissues (n = 10 per group). (**C, D**) Representative cytograms and quantitative analysis of CCR2^{+}Timd4^{-} macrophages in hearts (n = 10 per group). (**E, F**) Representative cytograms and quantitative analysis of Ly6G^{+} neutrophils in heart tissues (n = 10 per group). Data are expressed as mean ± SD. **P*<0.05. Data was analyzed using one-way ANOVA followed by Tukey's post-hoc analysis.

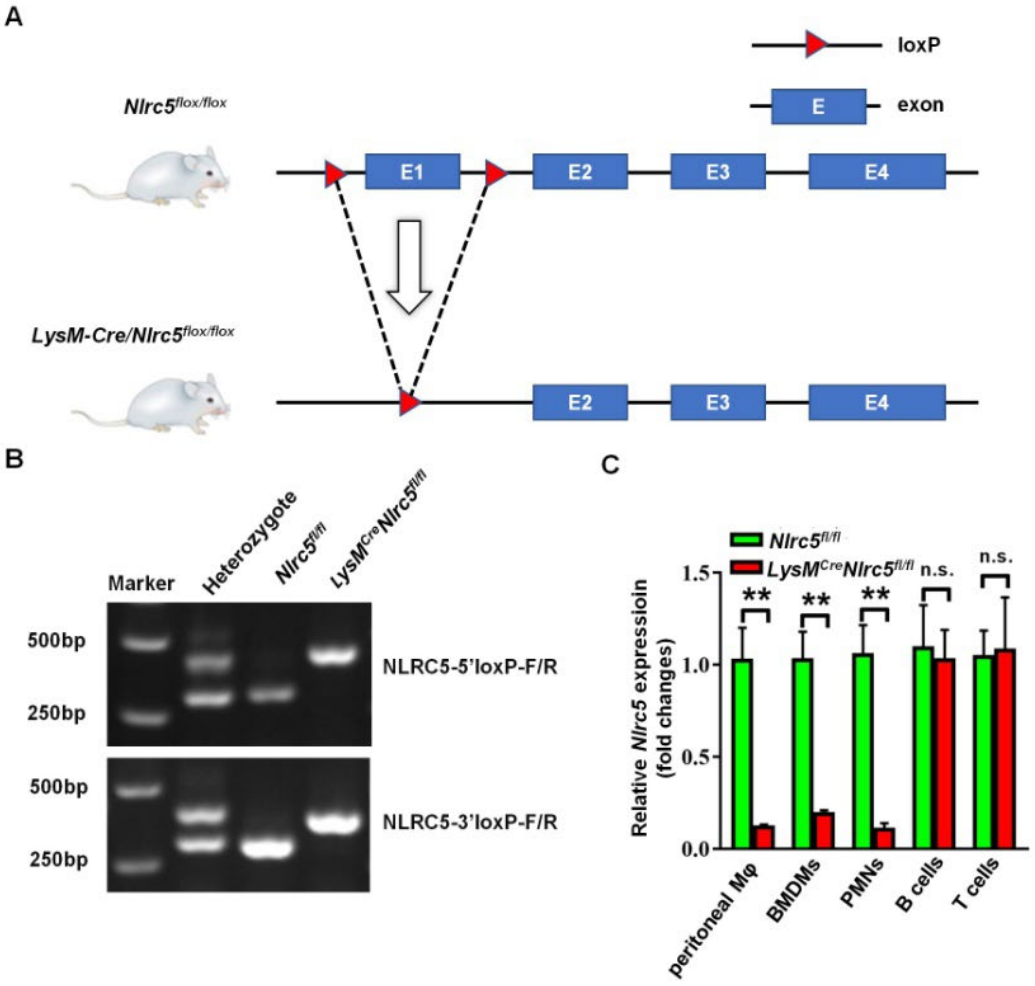

Supplemental Figure 10 Generation of *LysM-Cre/Nlrc5$^{flox/flox}$* mice. (**A**) Schematic diagram for establishing a line of *LysM-Cre/Nlrc5$^{flox/flox}$* mice. (**B**) Identification of *LysM-Cre/Nlrc5$^{flox/flox}$* mice by southern blot. (**C**) The mRNA expression of *Nlrc5* was quantified by real-time PCR in peritoneal macrophages (Mφ), peripheral blood neutrophils (PMNs), bone marrow-derived macrophages (BMDMs), splenic B cells and T cells from *Nlrc5$^{fl/fl}$* and *LysM-Cre/Nlrc5$^{flox/flox}$* mice. Data are expressed as mean ± SD. ***P*<0.01. Data was analyzed using Student's unpaired *t*-test.

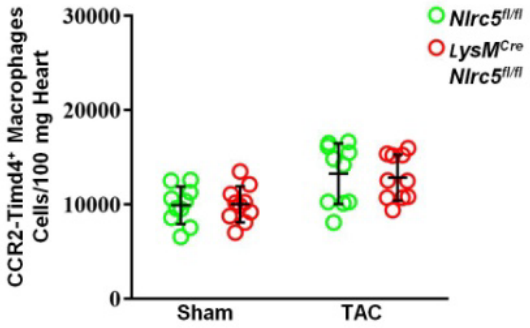

Supplemental Figure 11 Quantitative analysis of CCR2^{-}Timd4^{+} macrophages in heart tissues of control mice (*Nlrc5$^{fl/fl}$*) and macrophage-specific NLRC5 knockout mice (*LysM-Cre/Nlrc5$^{flox/flox}$*) after 1 week of TAC operation. n = 10 per group. Data are expressed as mean ± SD. Data was analyzed using one-way ANOVA followed by Tukey's post-hoc analysis.

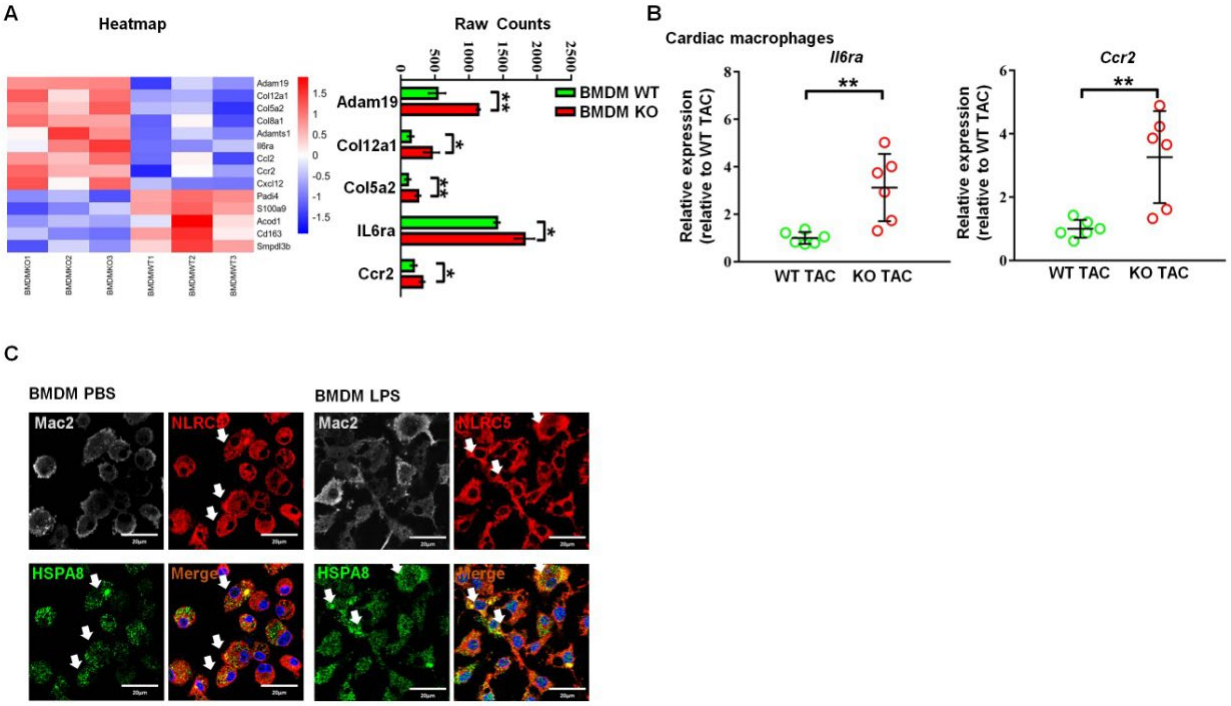

Supplemental Figure 12 Effect of HSPA8 knockdown on IKKβ and p38 phosphorylation. (**A**) Heatmap of WT and NLRC5 KO BMDM after RNA sequencing (n=3 per group) and raw counts analysis of the expression of several genes in BMDM of NLRC5 KO compared with WT from RNA-sequencing. (**B**) Relative mRNA expression of *Il6ra* and *Ccr2* in cardiac macrophages were assessed by real-time PCR. (**C**) Immunofluorescence staining of NLRC5 (red), Mac2 (grey), HSPA8 (green) and nuclei (blue) in BMDMs. Scale bars, 20 μm. Data are expressed as mean ± SD. **P*<0.05, ***P*<0.01. Data was analyzed using Student's unpaired *t*-test.

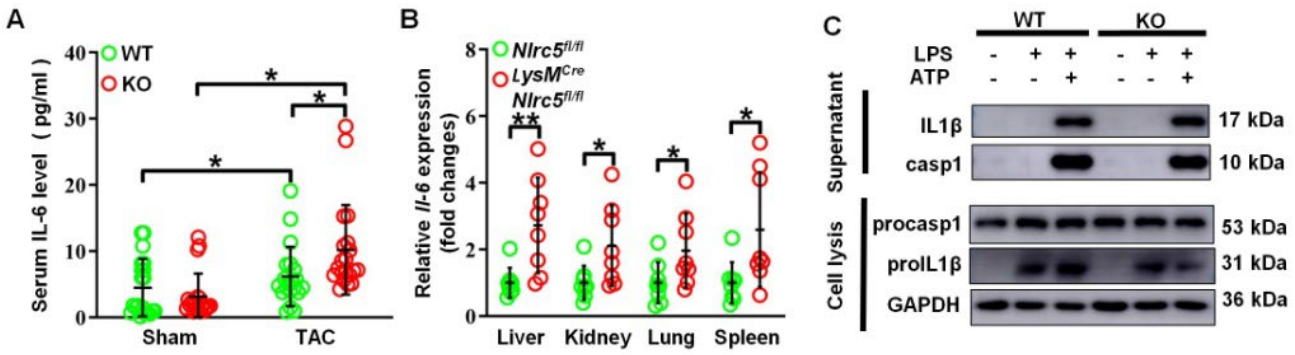

Supplemental Figure 13 The content of IL-6 in serum and different tissue in *Nlrc5$^{fl/fl}$* and *LysM-Cre/Nlrc5$^{flox/flox}$* mice after TAC. (**A**) The concentration of IL-6 (pg/ml) in serum of *Nlrc5$^{fl/fl}$* and *LysM-Cre/Nlrc5$^{flox/flox}$* mice after TAC was measured by ELISA kit (n = 20 per group). (**B**) Relative mRNA expression of *Il-6* in different tissues of *Nlrc5$^{fl/fl}$* and *LysM-Cre/Nlrc5$^{flox/flox}$* mice after TAC was quantified by real-time PCR (n = 8 per group). **(C)** Representative western blot images and quantitative analysis of protein expression in supernatants lysates and cell lysates of BMDMs from wild-type (WT) and *Nlrc5$^{-/-}$*(KO) mice treated with PBS or LPS (100 ng/mL) for 6 hours with subsequent stimulation with ATP (2.5 mmol/L) for 1 hour. Data are expressed as mean ± SD. **P*<0.05, ***P*<0.01. Data in panel (A) was analyzed using Kruskal–Wallis followed by Dunn's multiple comparison test. Data in panel (B) was analyzed using analyzed using Student's unpaired *t*-test.

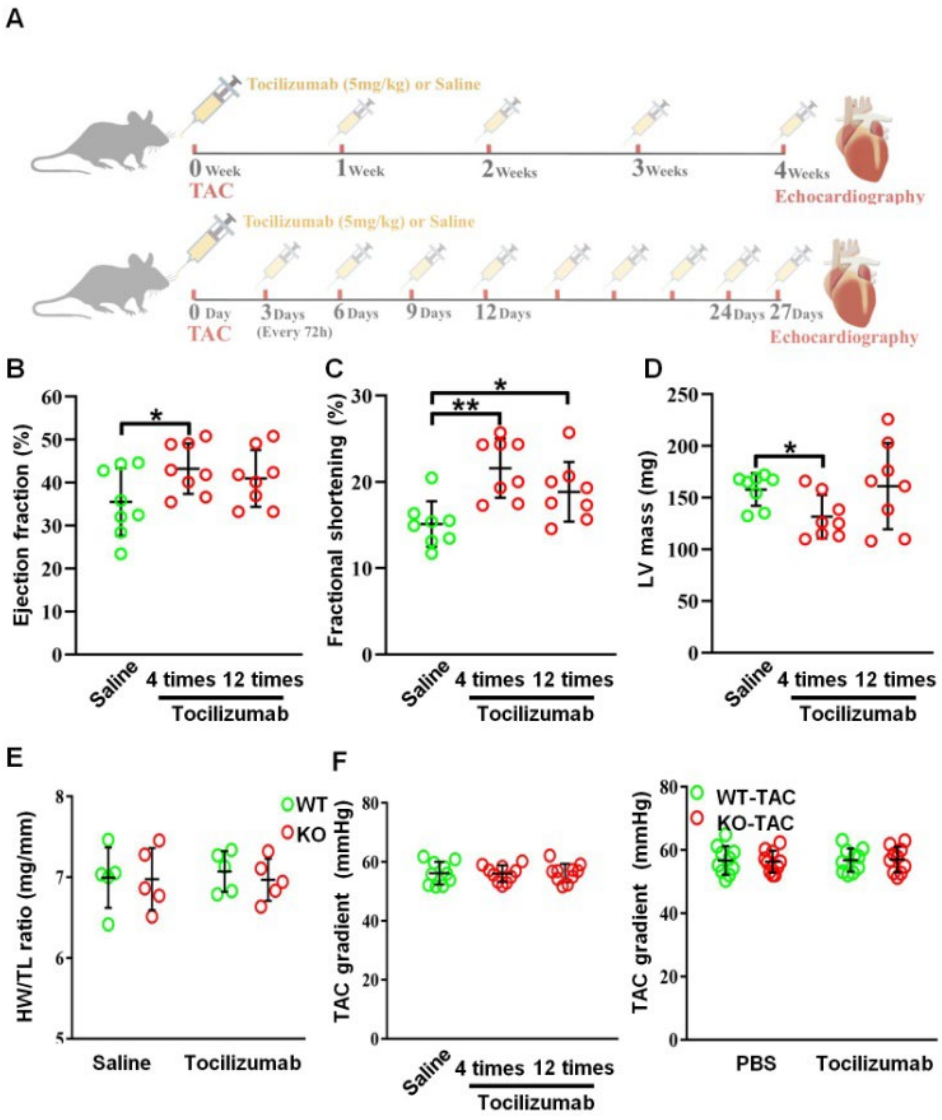

Supplemental Figure 14 Effect of different dosages of IL-6 receptor inhibitor Tocilizumab. (**A**) Experimental design. The IL-6 receptor inhibitor Tocilizumab (5mg/kg, once per week or every 72 hours, 4 weeks) was used for TAC-induced mice. (**B-D**) Echocardiographic analyses of ejection fraction (EF), fractional shorting (FS) and left ventricular (LV) mass in mice after 4 weeks of sham and TAC operation were shown (n = 8 per group). (**E**) The ratios of heart weight and body weight (HW/TL) in anti-IL-6 receptor treated mice (n = 5 per group). (**F**) Peak pressure gradient across the aortic constriction was measured 4 weeks after TAC or sham surgery (n=10 per group). Data are expressed as mean ± SD. **P*<0.05, ***P*<0.01. Data were analyzed using one-way ANOVA followed by Tukey's post-hoc analysis.

Supplemental Table 1: Basic characteristics of study population.

	Control (n=15)	HCM (n=15)	P value
Age, yrs	65.3 ± 7.2	61.1 ± 13.4	0.285
Male	11 (73.3)	14 (93.3)	0.367
Smoking (%)	6 (40.0)	9 (60.0)	0.370
Diabetes (%)	5 (33.3)	5 (33.3)	0.852
Hypertension (%)	12 (80.0)	9 (60.0)	0.202
EF (%)	60.47 ± 4.29	41.35 ± 5.56	**<0.001**
IVSd (mm)	9.87 ± 0.64	18.53 ±2.81	**<0.001**
LVPWd (mm)	9.47 ± 0.74	10.47 ± 0.87	**0.002**
E/e' (%)	10.33 ± 1.35	10.71 ± 1.16	0.407

Abbreviations: HCM, hypertrophic cardiomyopathy; EF, Ejection Fraction; IVSd, diastolic interventricular septum; LVPWd, diastolic left ventricular posterior wall; E/e', Early mitral inflow velocity to mitral annular early diastolic velocity ratio.

Supplemental Table 2: Summary of fluorescently labeled antibodies.

Antibody	Catalog	Dilution
BB515, anti-mouse CD45	BD Bioscience 564590	1:100
PE, anti-mouse CD11b	BD Bioscience 553311	1:100
BV421, anti-mouse F4/80	BD Bioscience 565411	1:100
APC, anti-mouse CCR2	R&D system FAB5538A	1:100
BV650, anti-mouse Ly6G	BD Bioscience 740554	1:100
PE-Cy7, anti-mouse Ly6C	BD Bioscience 552985	1:100
APC, anti-mouse CD45	BD Bioscience 559864	1:100
PE, anti-mouse CD3	BD Bioscience 553240	1:100
FITC, anti-mouse CD4	BD Bioscience 553729	1:100
PerCP/cy5.5, anti-mouse CD8	BD Bioscience 551162	1:100
PE-Cy7, anti-mouse MerTK	BioLegend 151521	1:100
PE, anti-mouse Timd4	BioLegend 130005	1:100
BV605, anti-mouse CD64	BioLegend 139323	1:100
PE, anti-human CD16	BioLegend 360703	1:100
BV421, anti-human CD45	BioLegend 304031	1:100
APC, anti-human CD14	BioLegend 301807	1:100

Supplemental Table 3: Summary of primer sequences for RT-PCR.

Gene	Primer sequence
NLRC5-Human	Forward: 5’ GCTCGGCAACAAGAACCTGT 3’
	Reverse: 5’ GGTCCAAGGTCTCGTTCCT 3’
NLRC1-Human	Forward: 5’ ACTGAAAAGCAATCGGGAACTT 3’
	Reverse: 5’ CACACACAATCTCCGCATCTT 3’
NLRC2-Human	Forward: 5’ CACCGTCTGGAATAAGGGTACT 3’
	Reverse: 5’ TTCATACTGGCTGACGAAACC 3’
NLRC3-Human	Forward: 5’ TCTCAGTGAAGAGGTCGAAGA 3’
	Reverse: 5’ GGCTGCTCAAGAAGAAATACG 3’
NLRC4-Human	Forward: 5’ TGCATCATTGAAGGGGAATCTG 3’
	Reverse: 5’ GATTGTGCCAGGTATATCCAGG 3’
NLRP1-Human	Forward: 5’ GCAGTGCTAATGCCCTGGAT 3’
	Reverse: 5’ GAGCTTGGTAGAGGAGTGAGG 3’
NLRX1-Human	Forward: 5’ CAGCGACCAGATGATCGTATC 3’
	Reverse: 5’ TGGTGGCGTATAAAGGCCCTA 3’
NLRCA-Human	Forward: 5’ CCTGGAGCTTCTTAACAGCGA 3’
	Reverse: 5’ TGTGTCGGGTTCTGAGTAGAG 3’
NLRP3-Human	Forward: 5’ GATCTTCGCTGCGATCAACAG 3’
	Reverse: 5’ CGTGCATTATCTGAACCCCAC 3’
GAPDH-Human	Forward: 5’ ACAACTTTGGTATCGTGGAAGG 3’
	Reverse: 5’ GCCATCACGCCACAGTTTC 3’
Nlrc5-Mouse	Forward: 5’ AGGCTCCCACTGCTTAGACA 3’
	Reverse: 5’ CGGACAGCAAGAGTTTCTCC 3’
Anp-Mouse	Forward: 5’ ATTGACAGGATTGGAGCCCAGAGT 3’
	Reverse: 5’ TGACACACCACAAGGGCTTAGGAT 3’
Bnp-Mouse	Forward: 5’ AGTCCTTCGGTCTCAAGGCA 3’
	Reverse: 5’ CCGATCCGGTCTATCTTGTGC 3’
Fibronectin-Mouse	Forward: 5’ ATGTGGACCCCTCCTGATAGT 3’
	Reverse: 5’ GCCCAGTGATTTCAGCAAAGG 3’
Collagen Iα-Mouse	Forward: 5’ GCTCCTCTTAGGGGCCACT 3’
	Reverse: 5’ ATTGGGGACCCTTAGGCCAT 3’
Hspa8-Mouse	Forward: 5’ CCAAGGTCCAAGTGGAATACAAA 3’
	Reverse: 5’ TCTTTCCGAGGTACGCTTCTG 3’
Il-6-Mouse	Forward: 5’ TAGTCCTTCCTACCCCAATTTCC 3’
	Reverse: 5’ TTGGTCCTTAGCCACTCCTTC 3’
Cxcl1-Mouse	Forward: 5’ CTGGGATTCACCTCAAGAACATC 3’
	Reverse: 5’ CAGGGTCAAGGCAAGCCTC 3’
Icam1-Mouse	Forward: 5’ GTGATGCTCAGGTATCCATCCA 3’
	Reverse: 5’ CACAGTTCTCAAAGCACAGCG 3’
Il-6r-Mouse	Forward: 5’ GCCACCGTTACCCTGATTTG 3’
	Reverse: 5’ TCCTGTGGTAGTCCATTCTCTG 3’
Gapdh-Mouse	Forward: 5’ TGACCTCAACTACATGGTCTACA 3’
	Reverse: 5’ CTTCCCATTCTCGGCCTTG 3’
Anp-Rat	Forward: 5’ GGGCTTCTTCCTCTTCCT 3’
	Reverse: 5’ TGAGACGGGTTGACTTCC 3’
α-SMA-Rat	Forward: 5’ GTCCCAGACATCAGGGAGTAA 3’
	Reverse: 5’ TCGGATACTTCAGCGTCAGGA 3’
Gapdh-Rat	Forward: 5’ ATGGGAAGCTGGTCAAC3’
	Reverse: 5’ GTGGTTCACACCCATCACAA 3’